Lipid Rafts and Cytoskeletal Proteins in Placental Microvilli Membranes from Preeclamptic and IUGR Pregnancies

Gloria Riquelme · Catalina Vallejos · Nicole de Gregorio · Bárbara Morales · Valeria Godoy · Macarena Berrios · Noelia Bastías · Carolina Rodríguez

Abstract Intrauterine growth restriction (IUGR) and preeclampsia (PE) are leading causes of perinatal and maternal morbidity and mortality. Previously we reported the expression of lipid rafts in classical microvillous membrane (MVM) and light microvillous membrane (LMVM), two subdomains in apical membrane from the human placental syncytiotrophoblast (hSTB), which constitute the epithelium responsible for maternal–fetal transport. Here the aim was to study the raft and cytoskeletal proteins from PE and IUGR. Microdomains from MVM and LMVM were tested with raft markers (placental alkaline phosphatase, lipid ganglioside, and annexin 2) and a nonraft marker (hTf-R). No changes were detected with those markers in whole purified apical membranes in normal, PE, and IUGR pregnancies; however, their patterns of distribution in lipid rafts were different in PE and IUGR. Cholesterol depletion modified their segregation, confirming their presence in lipid rafts, although unlike normal placenta, in these pathologies there is only one type of microdomain. Additionally, the cytoskeleton proteins actin, ezrin, and cytokeratin-7 showed clear differences between normal and pathological membranes. Cytokeratin-7 expression decreased to 50% in PE, and the distribution between LMVM and MVM ($\sim$43 and 57%, respectively) changed in both PE and IUGR, in contrast with the asymmetrical enrichment obtained in normal LMVM ($\sim$62%). In conclusion, lipid rafts from IUGR and PE have different features compared to rafts from normal placentae, and this is associated with alterations in the expression and distribution of cytoskeletal proteins.

Keywords Lipid rafts · Placenta · Preeclampsia · IUGR · Apical membrane · Cytoskeletal proteins

The human placental syncytiotrophoblast (hSTB) form an epithelial cell layer that is able to separate maternal and fetal blood, providing the main barrier to maternal–fetal exchange. To guarantee its function and to control material flow in one defined direction, the hSTB maintains a polarized organization with two distinct (apical and basal) plasma membrane domains. Previously, using differential sucrose density migration, we isolated and characterized two fractions from the apical (maternal-facing) membrane: the classical microvillous membrane (MVM) and another apical fraction, termed light microvillous membrane (LMVM). These fractions were obtained from both normal and preeclamptic placentae (Jimenez et al. 2004). As in other epithelial cells, the apical hSTB membrane is a specialized structure particularly rich in membrane lipids that are characteristic of lipid rafts (Godoy and Riquelme 2008; Paradela et al. 2005; Xu et al. 2006). These lipids seem to be essential for the maintenance and stability of microvilli (Meder et al. 2006). Several raft markers such as alkaline phosphatase, annexin 2 (Anx-2) and lipid ganglioside (GM1) have been found in microvillous rafts from different cell types including hSTB (Godoy and Riquelme 2008; Hanada et al. 1995; Harder and Gerke 1994; Harder et al. 1998). The methods to isolate and characterize the rafts are based on their resistance to solubilization by nonionic detergents (Brown and Rose 1992). Detergent-resistant membranes (DRMs) have proved to be a useful method to obtain microdomains (Hanada et al. 1995;

G. Riquelme (✉) · C. Vallejos · N. de Gregorio · B. Morales · V. Godoy · M. Berrios · N. Bastías · C. Rodríguez
Depto. de Fisiología y Biofísica, Instituto de Ciencias Biomédicas (ICBM), Facultad de Medicina, Universidad de Chile, Casilla 70005, Santiago 7, Chile
e-mail: griquelm@med.uchile.cl

Babiychuk et al. 2002; Schroeder et al. 1998). A large number of cell surface proteins are found in lipid rafts (Babiychuk et al. 2002; Chatterjee and Mayor 2001; Rajendran et al. 2003; Simons and Toomre 2000), although DRMs isolated using this technique are aggregates of raft domains and do not strictly represent the native state of lipid rafts in cell membranes (Lichtenberg et al. 2005).

We reported two distinguishable lipid raft subsets from MVM and LMVM isolated from normal placentae (PN). Both of these fractions are insoluble in Triton X-100 and sensitive to cholesterol depletion. Additionally, we showed that MVM and LMVM have different cholesterol contents and also differ with respect to their composition of cytoskeletal proteins such as actin, ezrin and cytokeratin-7 (CK-7). We found that actin and ezrin were significantly more abundant in MVM than in LMVM indicating that MVM might correspond to the microvillous core (finger-like projections). This region is composed of actin filaments and is stabilized by actin cross-linked proteins such as ezrin (Berryman et al. 1995). On the other hand, CK-7 expression was enhanced in LMVM as compared with MVM, suggesting that LMVM may correspond to the bottom part of the microvilli, which is linked to distinct cytoskeletal proteins such as the intermediate filament component, CK-7. Our findings suggest the existence of two distinct subdomains within the apical domains (Godoy and Riquelme 2008).

Lipid rafts participate actively in signal transduction and cellular adaptation to changing environments (Babiychuk et al. 2002; Chatterjee and Mayor 2001; Simons and Toomre 2000; Rajendran and Simons 2005) and many proteins responsible for membrane cellular transport have been reported to be present in raft domains (Brugger et al. 2007; Jahn and Braet 2008; Staneva et al. 2004). At present, numerous studies show that the partitioning of a protein into or out of a raft could be critical to the understanding of diverse pathologies (Fantini et al. 2002; Romanenko et al. 2004; Simons and Ehehalt 2002). We have focused our current studies on preeclampsia (PE), a pregnancy pathology considered to be one of the most significant health problems in human pregnancy, complicating 6–8% of all gestations over 20 weeks, (Huppertz 2008; Dekker and Sibai 1998) and intrauterine growth restriction (IUGR), which affects 8–14% of normotensive pregnancies. IUGR is believed to arise as a result of inadequate blood supply to the placenta and/or inadequate transport of nutrients across the placenta to the fetus (Cartwright et al. 2010). Despite continuous advances in research, the understanding of the pathophysiology of PE and IUGR remains a major challenge. Clinical diagnostic criteria of PE involve hypertension and proteinuria; however, it is a multisystemic disorder with a wide range of clinical presentations (Huppertz 2008; Taylor 1997; Than et al. 2008; Widmer et al. 2007). It is known that there are

many dysfunctions and morphological alterations in the preeclamptic and IUGR placentae (Afzal-Ahmed et al. 2007; Belkacemi et al. 2007; Lindheimer and Katz 1989; Nochy et al. 1986; Powers et al. 2008). Nevertheless, the molecular processes associated with the placental epithelium are still poorly understood.

Our aim has been to investigate transplacental transport and the relationship with its environment in normal (Godoy and Riquelme 2008; Bernucci et al. 2003, 2006; Diaz et al. 2008; Llanos et al. 2002; Riquelme and Parra 1999; Riquelme et al. 1995; Vallejos and Riquelme 2007), IUGR (Vallejos et al. 2010; Morales et al. 2009; De Gregorio et al. 2010) and preeclamptic placentae (Bernucci et al. 2003; Vallejos et al. 2010; De Gregorio et al. 2010). In 2003 we reported the first evidence of a functionally altered ionic channel protein in pathological hSTB by means of electrophysiological methods (Bernucci et al. 2003).

The purpose of the present study was to identify and characterize lipid rafts present in apical fractions from PE and IUGR hSTB and compare them with apical rafts from normal pregnancies. We also sought to explore the relationship between these pathological rafts and cytoskeleton proteins. As mentioned above, these relationships have been investigated in PN, and those results indicated that specific subdomain localization in the apical membrane could explain the differences between LMVM and MVM lipid raft composition. Because many functions of the apical membrane are based on membrane dynamics and structure–function correlation, apical rafts may play a role in mediating different intracellular mechanisms in the placental epithelial barrier that could directly relate to the pathological disorder. Although we could not clarify whether these disorders are causes or effects, we are convinced that the lipid microdomain characterization of the microvilli from PE and IUGR placentae and their connections with the cytoskeleton may be of great importance to our understanding of the molecular mechanisms behind the processes that occur in hSTB from pathological pregnancies.

Materials and Methods

Placenta Collection

Placentae obtained from normal pregnancies and from pregnancies presenting moderate PE and IUGR, were collected immediately after delivery from the San José Hospital Maternity Unit and transported to the laboratory on ice. Diagnosis of moderate PE was based on the classical criteria of systolic and diastolic blood pressure $\geq 140/90$ mm Hg on at least two occasions and proteinuria ≥ 300 mg/24 h. Patients with severe PE, defined as diastolic blood pressure >110 mm Hg and/or proteinuria

>5 g/day, were excluded from our study sample (Centro de Diagnóstico e Investigaciones Perinatales, Chile, http://www.cedip.cl/Guias/Guia2003/). Placentae from patients with HELLP syndrome were also excluded, as were placentae from patients with moderate PE accompanied by any other pathology. Diagnosis of idiopathic IUGR was established by the responsible physician via clinical estimation of fetal weight corresponding to a growth rate under the 10th percentile adjusted for sex and gestational age according to the standard curve (Ministry of Health of Chile) of intrauterine growth (Juez 1989). Fetuses that were above the 10th percentile but whose growth had stalled for a period of at least 14 days were also considered as IUGR. Exclusion criteria included: fetal or maternal infections, maternal drug or alcohol abuse, multiple pregnancies, fetal malformations, chromosomal abnormalities, maternal chronic hypertension, maternal cardiovascular or autoimmune disease, diabetes, and moderate PE. Placentae with IUGR from preeclamptic pregnancies were excluded. All of the placentae used came from term pregnancies.

Preparation of Placental Apical Membranes

Human placental apical or microvillous membrane (MVM) and LMVM vesicles were prepared from fresh placenta by a previously described method that enables simultaneous isolation of apical and basal membranes from the same placenta (Jimenez et al. 2004). The purification method included precipitation of nonmicrovillous membrane with magnesium ions, differential centrifugation and a sucrose step gradient; this assured that isolated fractions were enriched and free of contamination. All solutions were buffered with 20 mM Tris–maleate, pH 7.4. A portion (2–3 ml) of the microvillous-enriched preparation containing about 10–15 mg of protein was overlaid on the sucrose gradient. Bands were obtained at 10/37% and 37/45% sucrose interfaces, corresponding to LMVM apical fraction and to the classical MVM apical fraction, respectively. These fractions were collected and diluted 10-fold with 20 mM Tris–maleate, pH 7.4, before centrifugation at $110,000 \times g$ for 30 min. The final pellet was resuspended in 300 mM sucrose 20 mM Tris–maleate, pH 7.4 buffer, and stored in liquid nitrogen. Protein concentration was determined using a bicinchoninic acid protein assay kit (Pierce Biotechnology, Rockford, IL) for the colorimetric detection and quantification of total protein (Wiechelman et al. 1988; Smith et al. 1985). The purity and enrichment of the fractions were determined routinely by assaying for alkaline phosphatase activity, an apical membrane marker; adenylate cyclase, a basal membrane marker; and mitochondrial membrane markers (cytochrome c oxidase and succinate dehydrogenase). Enrichment of alkaline phosphatase activity was over 20-fold for MVM and LMVM;

both apical fractions were essentially free of basal membranes and mitochondrial membranes. The purity and cross-contamination of the membranes were similar to those previously observed (Jimenez et al. 2004).

Preparation of Apical Lipid Microdomains

Apical plasma membrane microdomains were isolated separately from MVM and LMVM enriched membrane fractions as DRMs through extraction with Triton X-100 using a modified protocol based on that described by Brown and Rose (1992). As we described in Godoy and Riquelme (2008), PN/PE/IUGR DRMs from isolated apical fractions (MVM and LMVM) were extracted with 1% Triton X-100 on ice, then subjected to ultracentrifugation and sucrose flotation. After centrifugation, the gradients were divided into 10 fractions (0.5 ml each) from the top of the gradient and the pellet (fraction 11) was resuspended in 0.5 mL MBS-buffered saline (25 mM morpholinoethanesulfonic acid [MES], 150 mM NaCl, pH 6.5) for subsequent analysis. Throughout this article, we use the terms "lipid microdomains" or "lipid rafts" to refer to the membrane material that floats on the sucrose gradient around the 5/35% interface (fractions 1–5).

Characterization of Apical Membrane Flotation Gradient Fractions

All flotation fractions from MVM and LMVM were characterized by specific markers for protein or lipid content. Placental alkaline phosphatase (PLAP) was used as a positive marker for apical lipid microdomain fractions and human transferrin receptor (hTf-R) was used as a nonraft marker. Additionally, we used another raft protein marker, Anx-2, and GM1 (Harder and Gerke 1994; Gaus et al. 2005; Danielsen and Hansen 2003; Babiychuk and Draeger 2000; van der Goot and Harder 2001).

Depletion of Membrane Cholesterol by Methyl-β-Cyclodextrin (mβ-CD) Treatment

Cyclodextrin treatment was carried out as described previously by Danielsen and Hansen (2003). Placental apical vesicles (0.6 mg of total protein) were incubated with 2% w/v mβ-CD in MBS buffer at 37°C for 30 min, and were centrifuged at $21,000 \times g$ for 2 h at 4°C. The pellet was resuspended in 1 ml of 1% Triton X-100 in MBS-buffered saline, and microdomain preparation was carried out as described above.

Immunohistochemistry

Tissue samples from PN, PE and IUGR placentae were rinsed in NaCl 0.9% and fixed in 1% buffered

paraformaldehyde at pH 7.4, for 10 h minimum. Subsequently, the tissue was rinsed five times in ice-cold phosphate-buffered saline (PBS) and dehydrated through a graded series of ethanol to xylene, embedded in paraffin, and cut into 4-μm-thick sections. Afterward, paraffin was removed in xylene and the sections were rehydrated by passage through graded ethanol and, finally, distilled water. Antigen retrieval treatment was performed for β-actin and ezrin with heat-induced epitope retrieval by using 0.1 M citrate buffer, pH 6.0 (preheated for 10–15 min) for 30 min in a steamer. After washing in PBS, the sections (both treated with heat-induced epitope retrieval and nontreated) were incubated for 1 h at room temperature with 4% bovine serum albumin (BSA) in PBS to block nonspecific binding. Tissue was then incubated for 2 h at room temperature with a monoclonal antibody raised against β-actin diluted 1:3000, a monoclonal antibody against ezrin diluted 1:1000 and a monoclonal antibody against CK-7 diluted 1:200 in 2% BSA in PBS. Negative control sections were treated similarly, except that primary antibodies were omitted. After rinsing the samples with PBS, tissue sections were incubated for 1 h at room temperature with Cy2 conjugated AffiniPure goat anti-mouse IgG (Jackson Immunoresearch) which was used as a secondary antibody diluted 1:200 in PBS. Sections were viewed using a Carl Zeiss Laser Scanning Systems Pascal Confocal Microscope and the Zeiss LSM 5 Image Browser.

Electrophoresis, Western Blot Testing, and Densitometric Analysis

All flotation gradient fractions were tested by sodium dodecyl sulfate–1polyacrylamide gel electrophoresis (SDS-PAGE) and immunoblotting. Aliquots of 50 μl each were incubated with 10% trichloroacetic acid, TCA, (v/v) for 30 min on ice and were centrifuged at $21,000 \times g$ for 30 min at 4°C. The pellet was resuspended in sample buffer, boiled for 5 min and sonicated for 30 min. For the cytoskeletal proteins β-actin, ezrin, and CK-7, 20 μg of total protein of LMVM and MVM was used. Routinely, all three proteins had been probed in membrane fractions isolated from the same placenta. These samples and the molecular weight marker (PageRuler Prestained Protein Ladder, Fermentas) were loaded on a 10% SDS polyacrylamide gel. Electrophoresis was performed at 100 V, and the gel was transferred to a nitrocellulose membrane (BioRad) for 2 h at 100 V. The nitrocellulose membrane was blocked for 2 h at room temperature with 3% nonfat milk in Tween/saline buffer (138 mM NaCl, 270 mM KCl, 0.05% Tween-20), and washed in Tween/saline buffer. Membranes were incubated with primary antibody for 2 h at room temperature. All antibodies were diluted as follows in distilled water: anti-PLAP 1:5000, anti-Anx-2 1:2000, anti-hTf-R 1:500, anti-ezrin 1:2000, anti-CK-7 1:500, anti-β-actin 1:5000. After washing with Tween/saline buffer, membranes

were incubated with specific horseradish peroxidise (HRP)-linked secondary antibody: anti-rabbit 1:5000 or anti-mouse 1:10,000, both diluted in Tween/saline buffer and incubated for 1 h at room temperature. Bands were detected with the enhanced chemiluminescence Western Blotting Analysis System (EZ-ECL, Biological Industries, Kibbutz Beit Haemek 25115, Israel). Protein content was quantified with ImageJ 1.43i (Wayne Rasband, National Institutes of Health).

Dot Blot

To measure the expressions levels of GM1 in each fraction, 3 μl of flotation gradient fractions were dot blotted on nitrocellulose membrane, dried for 1 h and blocked for 2 h with 3% BSA in PBS (128 mM NaCl, 2 mM KCl, 8 mM Na_2HPO_4, 2 mM K_2HPO_4, pH 7.2) at room temperature. Later, the membrane was incubated overnight with the HRP-conjugated cholera toxin β subunit (1:10,000) and detected with the ECL system. Densitometry analysis of dot blot bands was performed in ImageJ 1.43i (Wayne Rasband, National Institutes of Health).

Reagents and Antibodies

All chemicals were analytical grade. Buffers were made with distilled water, and pH values were determined at room temperature. The following antibodies were used: mouse monoclonal antibody against human alkaline phosphatase, PLAP (clone 836, Sigma, St. Louis, MO), β-actin (Clone: C4, Immuno), ezrin (clone 3C12, Zymed San Francisco California, CA), CK-7 (Santa Cruz Biotechnology), hTf-R (clone H68.4, Zymed) and rabbit polyclonal antibody to Anx-2 (Santa Cruz), and HRP-conjugated secondary goat anti-mouse (Amersham) and rabbit (Santa Cruz, Biotechnology). For detection of glycosphingolipid GM1 on dot blot, HRP-conjugated cholera toxin β subunit (Sigma) was used.

Statistical Analysis

Results are expressed as mean ± SD. Measures of statistical significance were obtained using the one-way ANOVA plus Bonferroni multiple comparison test and Student's t-test. A P-value of less than 0.05 was considered significant.

Results

MVM and LMVM from PN, PE, and IUGR Placentae

As shown in Table 1, there was no statistically significant difference between the protein concentration data from

Table 1 Comparison of the enrichment factor, protein concentration, and distributions of markers membrane in LMVM and MVM purified membranes from normal and pathological human term placenta

Characteristic	PN		PE		IUGR	
	LMVM	MVM	LMVM	MVM	LMVM	MVM
Factor enrichment PLAP[a]	23.7 ± 2.4	18.8 ± 2.5 (n = 7)	27.2 ± 5.5	24.6 ± 5.1 (n = 6)	31.1 ± 5.4	27.9 ± 4.7 (n = 5)
Protein concentration (mg/ml)	7.3 ± 1.7	6.9 ± 1.9 (n = 7)	6.3 ± 1.9	8.0 ± 0.3 (n = 6)	7.1 ± 1.6	5.2 ± 1.7 (n = 5)
Distribution[b]						
Anx-2 (%)	49.0 ± 8	51.0 ± 8 (n = 5)	45.0 ± 8	55.0 ± 8 (n = 5)	46.0 ± 3.3	54.0 ± 3.3 (n = 3)
GM1 (%)	46.0 ± 3	54.0 ± 3 (n = 3)	47.0 ± 7	53.0 ± 7 (n = 3)	57.0 ± 4.8	43.0 ± 4.8 (n = 3)
PLAP (%)	61.0 ± 13	39.0 ± 13 (n = 4)	46.0 ± 4.4	54.0 ± 4.4 (n = 5)	48.0 ± 2.6	52.0 ± 2.6 (n = 3)
hTf-R (%)	41.6 ± 8	58.4 ± 8 (n = 4)	43.5 ± 10.5	56.5 ± 10.5 (n = 4)	53.9 ± 3.2	46.1 ± 3.2 (n = 2)

[a] The enrichment factor was calculated as the ratio of activity in membrane fractions to that in the homogenate. Values are mean ± SD

[b] The values presented as percentages correspond to relative density of the mark present in each apical fraction, which was normalized by the sum of densities in both fractions (MVM + LMVM as 100%)

$n = 7$ preparations of PN, $n = 6$ preparations of placentae from preeclamptic pregnancies (PE) and $n = 5$ preparations of placentae from IUGR pregnancies. The total protein for LMVM and MVM were 3.2 ± 0.5 and 6.7 ± 2.1 mg/100 g of villous tissue respectively for a pool including normal and pathological placentae ($n = 7$, PN + PE + IUGR). The protein recovery in LMVM + MVM, expressed as percent relative to homogenate was 0.29, 0.25 and 0.31% for PN, PE and IUGR respectively, with the percentage for PN and PE similar to that reported by Jimenez et al. (2004). In summary, a preparation from 100 g of villous tissue yielded approximately 3 and 6 mg of purified membrane protein for LMVM and MVM respectively for placentae from PN, PE or IUGR pregnancies.

Microvillus enrichment from both apical membrane fractions (MVM and LMVM) was assessed using the enzymatic activity of PLAP, an epithelial apical membrane marker that is abundant in the syncytiotrophoblast microvillus membrane. The PLAP enrichment factors relative to the initial tissue homogenate are shown in Table 1, confirming the apical identity of both membranes. There were no significant differences in enrichment of PLAP activity between normal and pathological apical membranes. The PLAP enrichment activity of the purified apical membrane fractions from normal, preeclamptic and IUGR confirmed the apical identity of both membranes and the values were comparable to those reported previously for apical membrane purification (Jimenez et al. 2004; Roos et al. 2004). Additionally, Table 1 shows the expression distributions of PLAP, GM1, Anx-2, and hTf-R in LMVM and MVM apical subdomains as seen by Western blot. The values presented as percentage correspond to relative density of the mark present in each apical fraction, which was normalized by the sum of densities in both fractions (MVM + LMVM as 100%). No significant difference

between the distribution in LMVM and MVM was found in normal or pathological placentae.

Lipid Rafts in Microvilli from IUGR and PE Placentae

To obtain DRM fractions from LMVM and MVM from pathological placentae, we used the protocol described in Materials and Methods. Placental apical membranes were incubated with 1% Triton X-100, separated by flotation in a discontinuous sucrose gradient, and tested by Western and Dot blot with the following raft markers: PLAP, GM1, Anx-2 with hTf-R as a nonraft marker. Figure 1 shows the distribution of these markers in DRMs from pathological LMVM and MVM. As seen in Fig. 1a, PLAP in PE is enriched in fractions 2 and 3 with practically the same distribution seen in both LMVM and MVM. Only one peak was seen for both membrane fractions at 24.2 ± 6.1 and 26.4 ± 10.4 respectively, and there were no differences in the distribution of this marker between LMVM and MVM flotation gradient fractions. Additionally, the GM1 distribution pattern in preeclamptic DRMs was practically the same for both apical fractions with a single peak in the fractions corresponding to the pellet in LMVM and MVM (Fig. 1b). Also in Fig. 1a, b, the Western blot quantification of PLAP and GM1 show a symmetrical distribution of both LMVM and MVM. There were no differences in the distribution of those markers between LMVM and MVM flotation gradient fractions from IUGR. The PLAP distribution pattern does not show a clear peak, the higher values in the first five fractions were 12.8 ± 5 and 9.5 ± 3.5. These values were almost 50% less than in PE. In the case of GM1, no peak was detected in any fractions, and the values from the lipid rafts are comparable between PE and IUGR, and the peak in fraction 11 detected in PE is the only differences detected between them (Fig. 1b). Figure 1c shows the
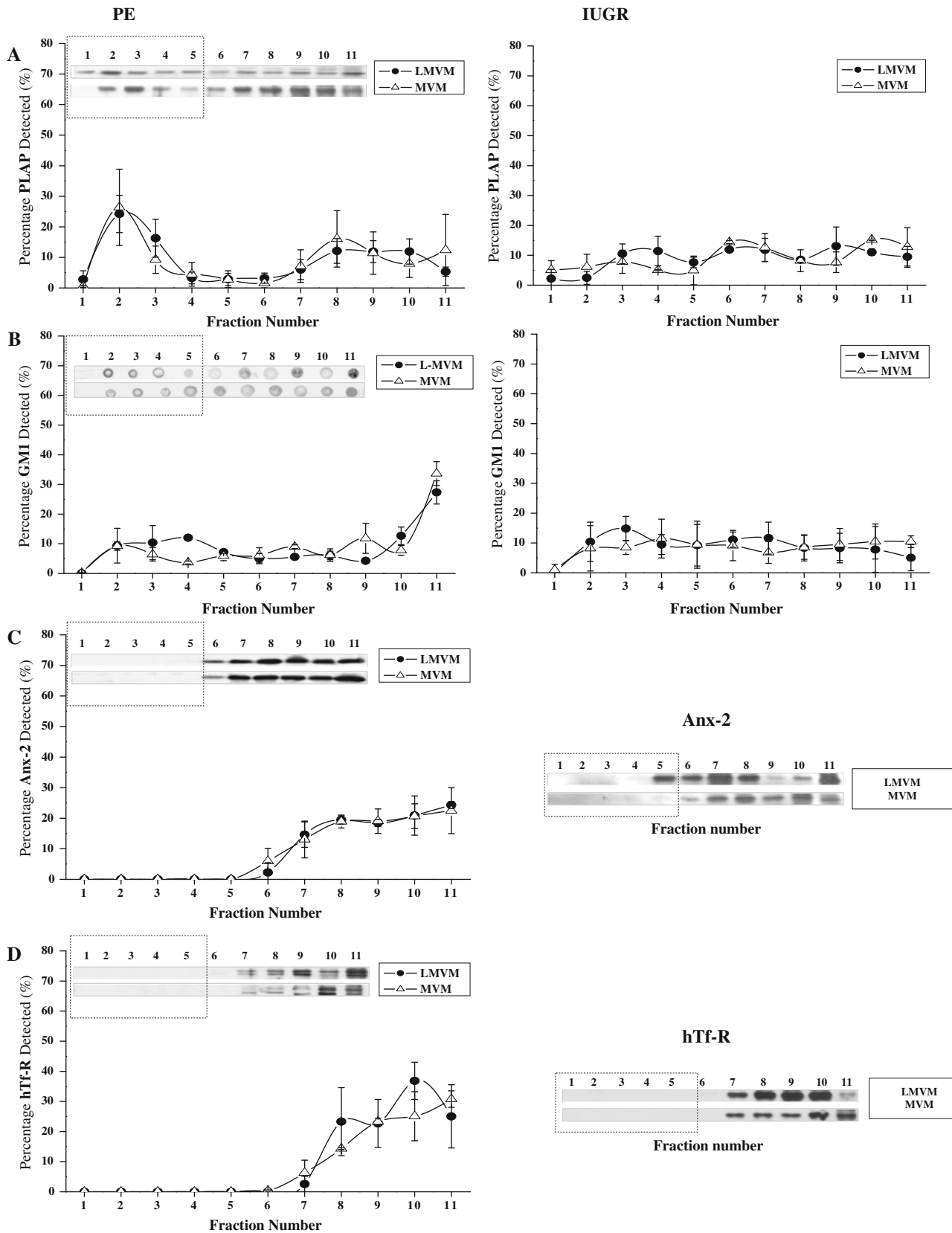
PE

IUGR

A

B

C

Anx-2

D

hTf-R

◀**Fig. 1** Distribution of typical raft markers in the flotation gradient fractions of LMVM and MVM from PE and IUGR placentae. Equal volumes of each sucrose gradient fraction of LMVM and MVM were separated by SDS-PAGE, transferred to a nitrocellulose membrane, and probed for PLAP, Anx-2 and hTf-R. The lipid GM1 was measure by Dot blot technique. The amount given is expressed as percentage of the sum of all fractions. Quantification of western blot analysis and representative image (*inset*) are shown for: **a** PLAP, **b** GM1, **c** Anx-2 and **d** hTf-R (no-raft marker). $n = 4$ PE placentae, $n = 5$ IUGR placentae, mean ± SD. Dotted box enclose the lipid rafts (fractions 1–5)

distribution of Anx-2, a protein associated with cholesterol and the cytoskeleton and linked to the cytoplasmic side of the membrane. Anx-2 was absent in the DRMs from both LMVM and MVM from preeclamptic and IUGR placentae. All of the bands (100% in PE and ∼90% in IUGR with, occasionally a band in fraction 5 of LMVM) appear in the soluble fractions, including the pellet fraction. This is, in contrast with our previous data, where this marker appears in the DRM fractions from normal LMVM (Godoy and Riquelme 2008).

To ensure that the DRM fractions were free of nonraft fractions, which could correspond to poorly solubilized complexes from the weak detergent treatment, we probed these fractions for hTf-R, a protein known to reside in nonraft areas. As Fig. 1d shows, this protein was not found in the fractions 1–6 in both LMVM and MVM from IUGR and PE placentae, indicating that those fractions were free of nonraft components.

The results described in Fig. 1 show no differences between the distribution of raft markers between flotation gradient fractions from pathological LMVM and MVM suggesting only one type of lipid raft for both membrane fractions. On the other hand, we have previously reported differential expression of microdomains (lipid rafts) in both MVM and LMVM purified microvillous membranes from normal placental human hSTB (Godoy and Riquelme 2008). Additionally, the pattern obtained for pathological lipid rafts are different in LMVM and MVM as compared to PN. These finding strongly suggest that lipid raft microdomains of pathological placentae are altered compared with those from PN.

Cholesterol-Depletion Effects on the Distribution of Raft Markers: DRMs from LMVM and MVM of PE and IUGR Placentae

Cholesterol depletion affects the associations of raft markers with DRM fractions in different ways. To establish a relationship between cholesterol content and raft marker association, we removed cholesterol from LMVM and MVM membranes by treating them with mβ-CD, a specific cholesterol removal agent (Danielsen and Hansen 2003) as described in Materials and Methods. As shown in Fig. 2a,
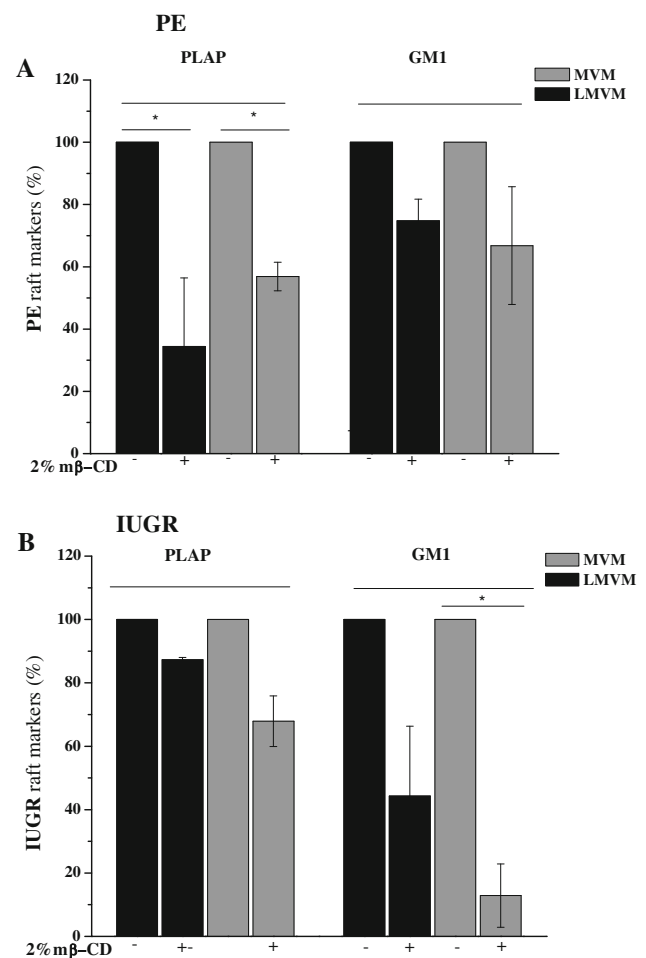

Fig. 2 Effect of cholesterol depletion on raft-markers association with DMRs of LMVM and MVM from PE and IUGR placentae. **a, b** The effect of cholesterol-depletion on PLAP and GM1 association with flotation gradient fractions from PE and IUGR apical membranes (LMVM and MVM). The percentage shown corresponds to the sum of relative density in fraction 1 to 5 of each apical membrane, controls and fractions preincubated with 2% mβ-CD (100% was the sum of 5 first fractions without treatment with mβ-CD). PLAP$_{PE}$ $n = 3$, GM1$_{PE}$ $n = 4$, PLAP$_{IUGR}$ $n = 3$ and GM1$_{IUGR}$ $n = 3$ (mean ± SEM, *$P < 0.05$)

PLAP association with DRM fractions from preeclamptic LMVM and MVM were significantly decreased by 2% mβ-CD treatment; however, PLAP association with DRM fractions from IUGR MVM was not affected by the removal of cholesterol (Fig. 2b). In both pathologies, PE and IUGR, GM1 association was decreased by mβ-CD treatment but that association was significantly affected in IUGR (Fig. 2a, b).

Cytoskeletal Proteins in Microvilli Membranes from Preeclamptic and IUGR Placentae: Differential Expression

Placental tissue samples and purified membranes (LMVM and MVM) from normal and pathological placentae were
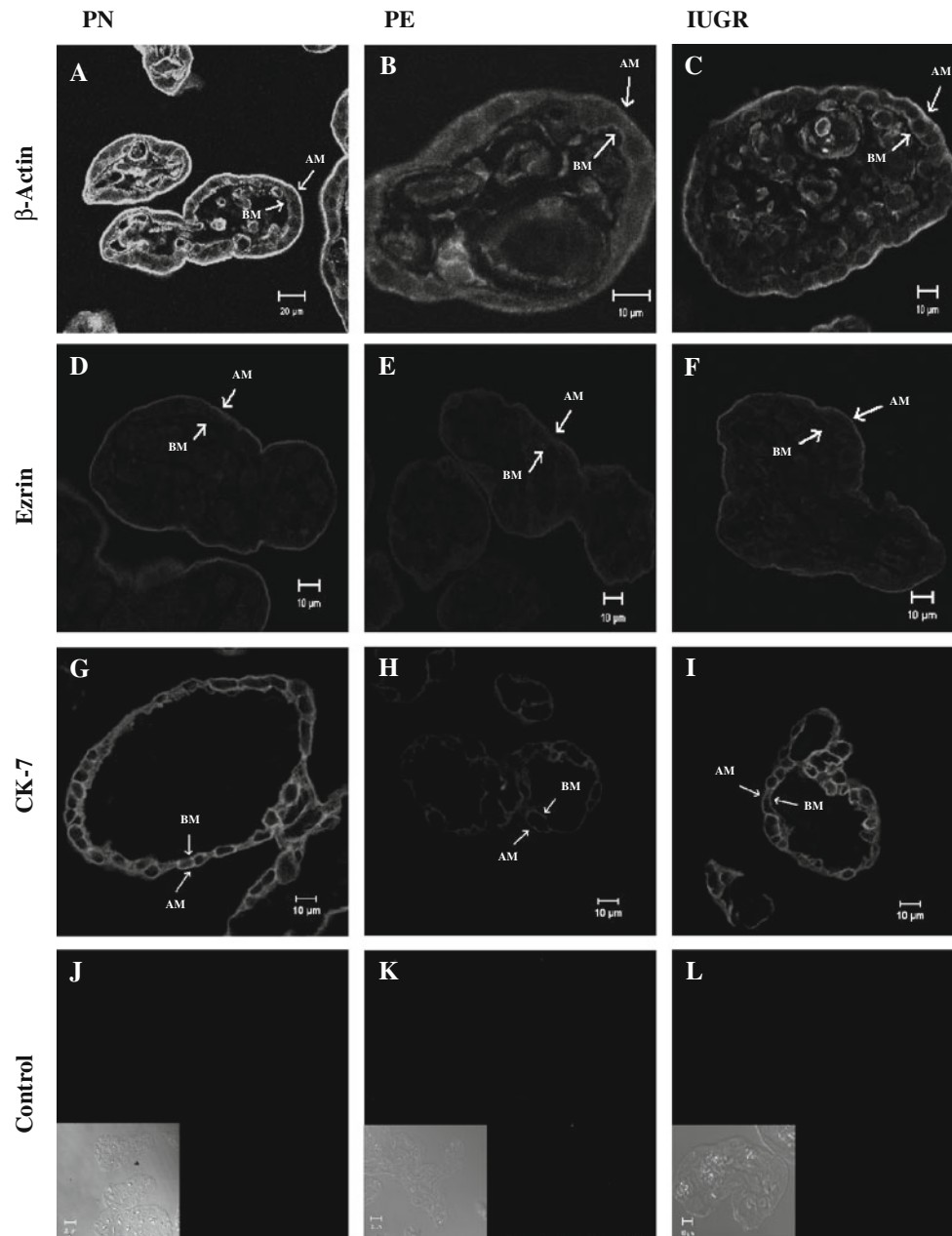
Fig. 3 Detection of actin, ezrin, and CK-7 in samples tissues from PN, PE, and IUGR placentae. Confocal fluorescence micrographs of immunohistochemical sections of placental villous tissue using primary antibodies against: β-actin (**a–c**), ezrin (**d–f**) and CK-7 (**g–i**) from PN (**a**, **d**, **g**, **j**), PE (**b**, **e**, **h**, **k**) and IUGR (**c**, **f**, **i**, **l**) placentae. **j–l** Control tissue using only secondary antibody (without primary antibody) with their respective transmitted light micrographs (*insets*). *AM* apical membrane, *BM* basal membrane

analyzed for three cytoskeletal proteins: β-actin, ezrin, and CK-7, which are localized in different parts of the cytoskeletal apical domain (Tyska et al. 2005; Wald et al. 2005; Morales et al. 2004; Berryman et al. 1995).

Placental tissue samples from normal, preeclamptic and IUGR pregnancies were treated with standard histological techniques with a specific antibody for β-actin, ezrin, and CK-7. The results show that these markers are more highly immuno localized in the apical membrane in all of the placentae examined ($n = 9$, PN + PE + IUGR) (Fig. 3). There were no apparent differences in the intensity of ezrin immunostaining in membranes of normal and pathological placentae ($n = 3$ independent placenta for each condition, PN, PE and IUGR). However, there was a large difference in the intensity of CK-7 in PE. These finding were confirmed when all three proteins were probed in membrane fractions isolated from PN, PE and IUGR placentae. The band associated with MVM + LMVM from PN was set as

100%. In this context, the presence of CK-7 from PE decreased to 51% and to 84% in IUGR in agreement with the results in Fig. 3. No changes were detected for ezrin and in the case of actin; the values were 100, 82 and 79% for PN, PE and IUGR respectively. We also investigated the distribution of these proteins in the apical subdomains (LMVM and MVM). The values are presented as a percentage corresponding to the relative density of the mark present in each apical fraction, which was normalized by the sum of densities in both fractions. Actin, ezrin and CK-7 showed differential expression between LMVM and MVM and were statistically significant in the three conditions (PN, PE, IUGR) tested. As shown in Fig. 4a, b, the expression of actin and ezrin were higher in MVM than in LMVM, while CK-7 showed an altered pattern between the fractions from normal and pathological placentae. As seen in Fig. 4, CK-7 protein was significantly more associated with LMVM than MVM in PN in agreement with previous results reported by Godoy and Riquelme (2008). This data is in contrast to the results in PE and IUGR placentae, where CK-7 was significantly more associated with MVM

than LMVM. This latter finding could support the differences observed between the lipid microdomains of normal and pathological placentae.

Distribution of Cytoskeletal Proteins in the DRMs from Normal and Pathological LMVM and MVM

Figure 5 shows the distribution of actin and ezrin between LMVM and MVM flotation gradient fractions isolated from PN, PE and IUGR placentae. No differences were observed for ezrin; this protein resides in nonraft areas in LMVM and MVM in all the conditions. Actin resides in nonraft areas for both normal MVM and LMVM subdomains. However, for IUGR and PE, the distribution of the bands was different for MVM and LMVM. In the case of CK-7, the results were inconclusive (data not shown). In some experiments there was segregation in lipid rafts, but with a variable pattern was not reproducible under specific conditions in either normal or pathological placentae.
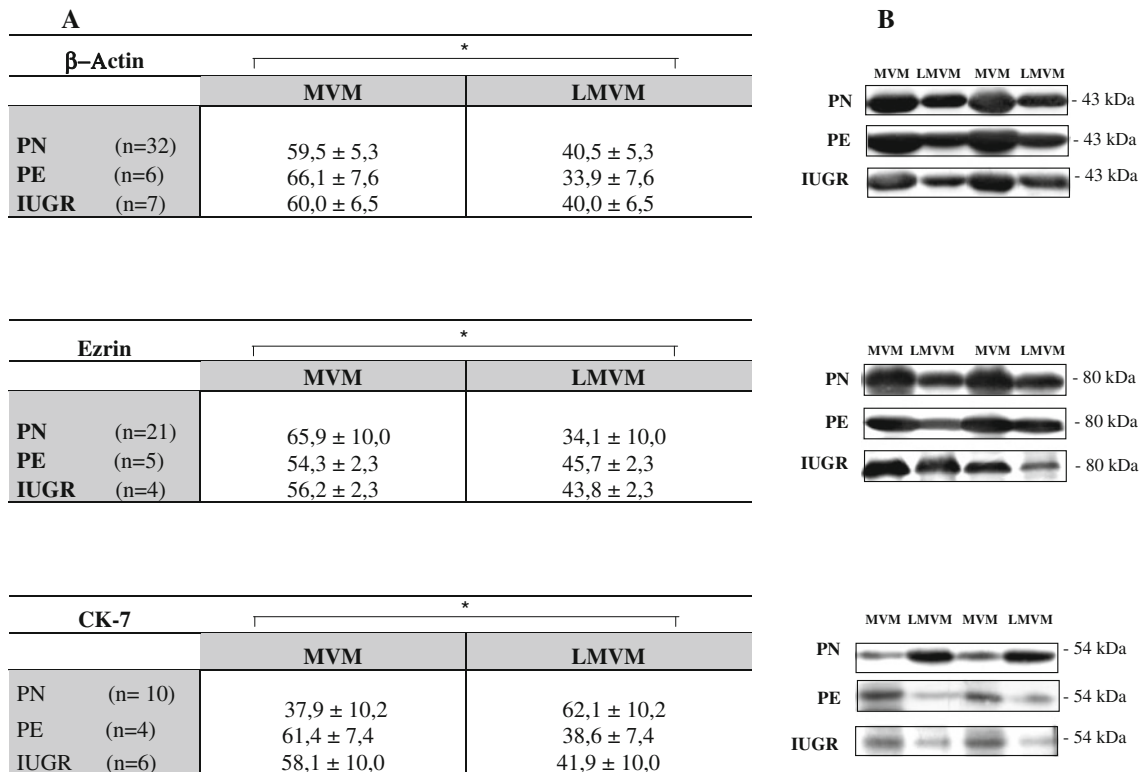
A

β–Actin	* MVM	* LMVM
PN (n=32)	59,5 ± 5,3	40,5 ± 5,3
PE (n=6)	66,1 ± 7,6	33,9 ± 7,6
IUGR (n=7)	60,0 ± 6,5	40,0 ± 6,5

Ezrin	* MVM	* LMVM
PN (n=21)	65,9 ± 10,0	34,1 ± 10,0
PE (n=5)	54,3 ± 2,3	45,7 ± 2,3
IUGR (n=4)	56,2 ± 2,3	43,8 ± 2,3

CK-7	* MVM	* LMVM
PN (n= 10)	37,9 ± 10,2	62,1 ± 10,2
PE (n=4)	61,4 ± 7,4	38,6 ± 7,4
IUGR (n=6)	58,1 ± 10,0	41,9 ± 10,0

B

Fig. 4 Expression and distribution of cytoskeletal proteins in LMVM and MVM from PN, PE, and IUGR placentae. **a** Distribution of β-actin, ezrin, and CK-7 tested in MVM and LMVM fractions from PN, PE, and IUGR placentae. The values, presented as percentages, correspond to relative density of the mark present in each apical fraction, which was normalized by the sum of densities in both fractions (MVM + LMVM as 100%). In all cases, significant differences were found for β-actin, ezrin, and CK-7 between MVM and LMVM fractions from PN, PE, and IUGR placentae (mean ± SD, *P < 0.05). **b** Representative western blot test for the cytoskeletal proteins tested in LMVM and MVM purified membranes from normal and pathological placenta
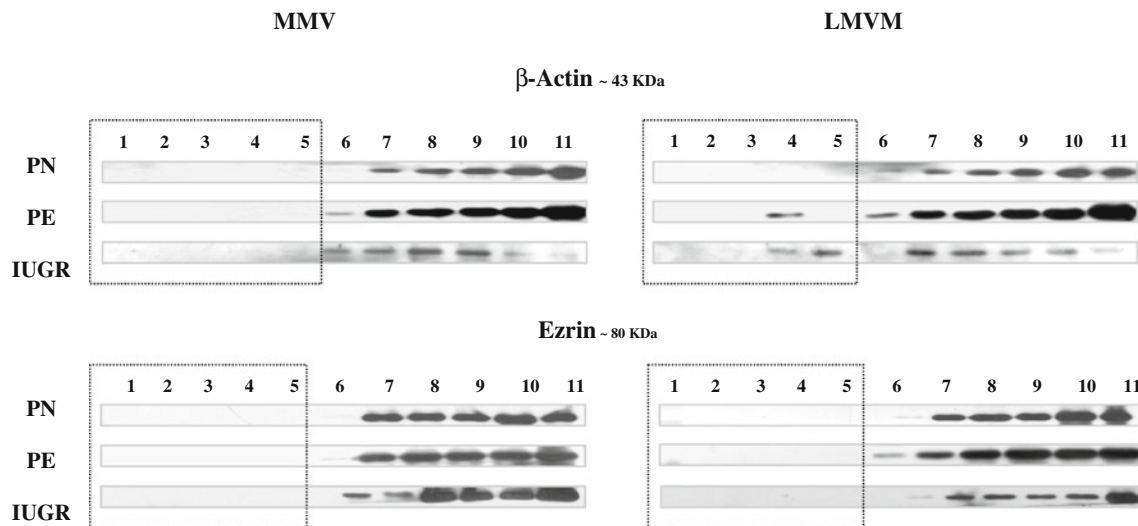
Fig. 5 Differential cytoskeletal protein distribution in the flotation gradient fractions of normal, preeclamptic, and IUGR LMVM and MVM subdomains. Representative western blot for actin (*top*) and ezrin (*bottom*), corresponding to DRMs of both MVM and LMVM from PN ($n = 6$), PE ($n = 4$), and IUGR ($n = 3$) placentae (*$P < 0.05$)

Discussion

The present study describes the presence of lipid rafts in both subdomains of apical membranes (LMVM and MVM) from hSTBs of complicated pregnancies: PE and IUGR. This study was performed using DRMs, cholesterol-sensitive depletion, and raft and nonraft markers to examine microdomain organization in the microvilli fractions. Our results showed that the lipid rafts from pathological tissue were significantly different from those reported in microvilli fractions from PN (Godoy and Riquelme 2008). Unlike the PN for which we reported two distinguishable lipid rafts subsets from MVM and LMVM, here we show both PE and IUGR have only one type of lipid raft with features common to both apical membrane fractions (LMVM and MVM). Furthermore we found that, in pathological placentae, the polarization of the cytoskeleton proteins in LMVM and MVM was different from that observed in PN. In PN, cytoskeleton protein distribution between LMVM and MVM supported the existence of two subdomains that correspond to specific microvilli regions (LMVM and MVM), asymmetry that could be the origin of the two types of rafts with the different properties detected. In the present paper we demonstrate that in pathological placentae this situation changes, there is only one type of raft and the expression and distribution of cytoskeletal proteins is altered.

One Type of Lipid Raft in LMVM and MVM from Pathological Placentae

The analysis of sucrose density gradient fractions with three raft markers (PLAP, Anx-2, and GM1) and hTf-R, a nonraft marker (Harder and Gerke 1994), allowed us to characterize the DRMs from both purified apical fractions for PE and IUGR together with PN as control, obtaining an equal distribution in the flotation gradient fractions from MVM and LMVM in both pathologies. On the other hand, hTf-R was totally absent from LMVM and MVM DRMs, indicating that the presence of raft markers in the six first fractions was not due to contamination from nonraft zones. Subsequently, we can say that both purified LMVM and MVM from pathological hSTB membranes presented sphingolipid/cholesterol-enriched membrane microdomains characterized by their resistance to detergent extraction and their ability to float in density gradient centrifugation, with only one type of lipids raft for both subdomains. On the other hand, the PLAP and GM1 distribution pattern in pathological DRMs was practically the same for both LMVM and MVM in each pathology. These results differ from those obtained previously with PN, where the PLAP and GM1 distribution was significantly different between flotation gradient fractions from LMVM and MVM. DRMs of LMVM from PN have a higher peak of PLAP and GM1 than is seen in the corresponding fractions from MVM (Godoy and Riquelme 2008). The peak of PLAP from IUGR LMVM and the peak of GM1 from LMVM PE and IUGR were notably less than that in normal LMVM. In DRMs from pathological LMVM, GM1 was reduced to around 54% in the peak fraction relative to respective fractions from PN. The data reported previously for PN was 26.4 ± 1.9, in contrast with 12.03 ± 0.5 obtained in pathological placentae.

Different Characteristics of Lipid Rafts in LMVM and MVM from PE and IUGR

In PE, PLAP association with DRM fractions was almost double that in IUGR and was significantly affected by mβ-CD treatment while DRM fractions from IUGR were not affected by the removal of cholesterol. In the case of GM1 no significant differences were detected in its distribution between lipid rafts from PE and IUGR; however, the cholesterol sensitivity was distinct. The association of GM1 with DRM fractions from IUGR was significantly affected by mβ-CD treatment, and in PE this association was weakly affected by the removal of cholesterol.

In summary, the symmetrical distribution pattern of raft markers suggest the presence of one type of lipid raft for both apical membrane fractions (LMVM and MVM) from PE and IUGR placentae in contrast with the PN (Godoy and Riquelme 2008). However, the data mentioned above suggest that differences exist between lipid rafts from PE and IUGR.

Cytoskeleton Proteins from Pathological hSTB Membranes

We demonstrated that proteins involved in the specialized cytoskeleton that stabilizes the microvilli of the syncytium, actin, ezrin and CK-7, have different characteristics in LMVM and MVM from pathological placentae compared to PN. The most remarkable change was with CK-7, (a component of the intermediate filaments in whole trophoblast epithelia) (Muhlhauser et al. 1995). The expression was considerably lower in membranes from PE compared with PN as shown by immunohistochemical staining of placental sections and Western blotting with purified membranes from PE. Additionally, CK-7 was significantly more associated with MVM than LMVM in PE, while in PN was the opposite and was more associated with LMVM than MVM. Our controls in PN were comparable to previous results reported by Godoy and Riquelme (2008). Similar trends were observed for IUGR, but the differences were more moderate. Ezrin and β-actin (both proteins are coupled with the microvillous finger-like projections region) from pathological membranes maintained a distribution similar to PN where both proteins are associated with MVM and LMVM; however, for ezrin, the differences between them was weakest compared with the difference in PN. Cytoskeletal proteins in pathological placentae could cause both PE and IUGR to have microdomains from apical fractions that differ from microdomains described previously in PN apical fractions. These findings suggest that in the purified apical fractions obtained, MVM and LMVM from pathological placentae display changes, at least in part, in the structural distinctions between the subdomains present in the microvilli membrane of the apical domain of hSTB as compared to that described during normal pregnancy (Fig. 6).

In agreement with other studies (Chichili and Rodgers 2007; Berryman et al. 1995) we previously proposed that cytoskeletal factors are involved in organization of apical rafts, and that specific subdomain localization in the microvillus contributes to the differences between LMVM and MVM lipid raft composition that we observed in PN (Godoy and Riquelme 2008). This is likely to also be applicable in the case of pathological placentae. In agreement with this hypothesis, it seems reasonable that our current data may explain the presence of altered lipid rafts

Fig. 6 Tentative model of the possible consequence of the distribution alterations of cytoskeletal protein in the microvillus from pathological hSTB. (**A**) PN.
(a) Actin$_{MVM} \gg$ Actin$_{LMVM}$.
(b) Ezrin$_{MVM} \gg$ Ezrin$_{LMVM}$.
(c) CK-7$_{MVM} \ll$ CK-7$_{LMVM}$.
(d) Expression of two distinguishable lipid rafts in both MVM and LMVM.
(**B**) Pathological placentae.
(a) Actin$_{MVM} \gg$ Actin$_{LMVM}$.
(b) Ezrin$_{MVM} >$ Ezrin$_{LMVM}$.
(c) CK-7$_{MVM} \gg$ CK-7$_{LMVM}$.
(d) Expression of only one type of lipid rafts both MVM and LMVM and with characteristics different to those from PN
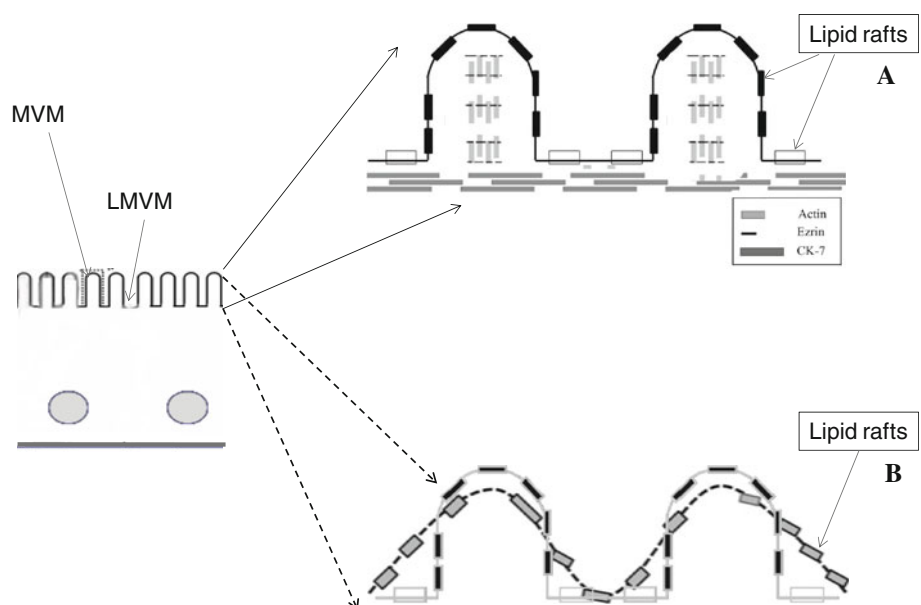
in both of these pathological apical fractions. The data described here could be especially significant because it appears that many functions of the apical membrane involve the presence of apical rafts. Their altered expression in hSTB from PE and IUGR pregnancies may therefore contribute to the dysfunctions observed in cellular physiological processes such as placental transport in these pathologies (Belkacemi et al. 2007; Carrera et al. 2003; Marin et al. 2008; Norberg et al. 1998; Jansson et al. 1998; Johansson et al. 2003; Cetin and Alvino 2009). In particular, we have reported altered ion currents in human placentae membranes from PE and IUGR pregnancies (Bernucci et al. 2003; Morales et al. 2009; Vallejos et al. 2010; De Gregorio et al. 2010). These channels displayed modified biophysical characteristics with respect to channels from PN (Bernucci et al. 2003). The question of why these channels are functionally modified in this pathology needs to be further addressed.

At the morphological level, alterations of the villous trophoblast have been described in the villous arrangement between placentae from normal and pathological pregnancies (Sibley et al. 2002; Guller et al. 2008; Huppertz et al. 2006a). The process of generating knots from the syncytiotrophoblast has been related to pregnancy pathologies such as IUGR and PE (Huppertz et al. 2006a). The increase in syncytial apoptosis in both pathologies has also been related to disruption in the microvilli (Huppertz et al. 2006a, b; Guller et al. 2008). The glycocalyx (oligosaccharides of varying complexity linked to membrane associated lipids and proteins) shows focal deformity on the surface of microvilli by electron microscopy in PE (Jones and Fox 1980), and the increase of syncytiotrophoblast glycogen in PE indicates a regression to a more immature trophoblast phenotype (Arkwright et al. 1993).

On the other hand, Tyska et al. (2005) have demonstrated changes and redistribution in the cytoskeletal proteins in enterocytes from myosin knockout mice that exhibit significant defects in microvillar membrane morphology. Myosin provides the lateral links between the plasma membranes and the core actin filaments in the microvilli of intestinal cells. When myosin was removed, the microvilli showed a pronounced lack of general organization, loosening their packing (Mooseker 1985). The protein composition of the cytoskeleton from hSTB apical membranes is different from that of intestinal apical membranes (Bretscher 1991). Ezrin is a major protein component of placental microvilli as reported by Berryman et al. (1995), and much of it is associated with the microvillus core (finger-like projections). This region is composed of actin filaments stabilized by ezrin an actin cross-linking protein. Change in this protein is most likely reflected in the architecture and morphology of the microvilli (Berryman et al. 1995). In our case, actin and

ezrin distribution suggests some changes in the purified fractions from apical membranes of pathological placentae compared to normal tissue. Additionally, our results obtained for CK-7 are in agreement with those recently reported by Ahenkorah et al. (2009), who demonstrated that at least five cytokeratins are present in the villous trophoblast and four of them were down-regulated in PE, suggesting that the preeclamptic microvilli has a weaker cytoskeleton.

In conclusion our present data demonstrated that, in the case of PE and IUGR, MVM and LMVM apical fractions could be less distinct than the specific regions such as the finger-like projections or the bottom part of the microvilli that have been proposed in the PN. This situation could explain the unique types of lipid rafts obtained for each pathology (Fig. 6).

References

Afzal-Ahmed I, Mann GE, Shennan AH, Poston L, Naftalin RJ (2007) Preeclampsia inactivates glucose-6-phosphate dehydrogenase and impairs the redox status of erythrocytes and fetal endothelial cells. Free Radic Biol Med 42:1781–1790

Ahenkorah J, Hottor B, Byrne S, Bosio P, Ockleford CD (2009) Immunofluorescence confocal laser scanning microscopy and immuno-electron microscopic identification of keratins in human materno-foetal interaction zone. J Cell Mol Med 13:735–748

Arkwright PD, Rademacher TW, Dwek RA, Redman CW (1993) Preeclampsia is associated with an increase in trophoblast glycogen content and glycogen synthase activity, similar to that found in hydatidiform moles. J Clin Invest 91:2744–2753

Babiychuk EB, Draeger A (2000) Annexins in cell membrane dynamics. Ca(2+)-regulated association of lipid microdomains. J Cell Biol 150:1113–1124

Babiychuk EB, Monastyrskaya K, Burkhard FC, Wray S, Draeger A (2002) Modulating signaling events in smooth muscle: cleavage of annexin 2 abolishes its binding to lipid rafts. FASEB J 16:1177–1184

Belkacemi L, Bainbridge SA, Dickinson MA, Smith GN, Graham CH (2007) Glyceryl trinitrate inhibits hypoxia/reoxygenation-induced apoptosis in the syncytiotrophoblast of the human placenta: therapeutic implications for preeclampsia. Am J Pathol 170:909–920

Bernucci L, Umana F, Llanos P, Riquelme G (2003) Large chloride channel from pre-eclamptic human placenta. Placenta 24: 895–903

Bernucci L, Henriquez M, Diaz P, Riquelme G (2006) Diverse calcium channel types are present in the human placental syncytiotrophoblast basal membrane. Placenta 27:1082–1095

Berryman M, Gary R, Bretscher A (1995) Ezrin oligomers are major cytoskeletal components of placental microvilli: a proposal for their involvement in cortical morphogenesis. J Cell Biol 131:1231–1242

Bretscher A (1991) Microfilament structure and function in the cortical cytoskeleton. Annu Rev Cell Biol 7:337–374

Brown DA, Rose JK (1992) Sorting of GPI-anchored proteins to glycolipid-enriched membrane subdomains during transport to the apical cell surface. Cell 68:533–544

Brugger B, Krautkramer E, Tibroni N, Munte CE, Rauch S, Leibrecht I, Glass B, Breuer S, Geyer M, Krausslich HG, Kalbitzer HR, Wieland FT, Fackler OT (2007) Human immunodeficiency virus type 1 Nef protein modulates the lipid composition of virions and host cell membrane microdomains. Retrovirology 4:70

Carrera F, Casart YC, Proverbio T, Proverbio F, Marin R (2003) Preeclampsia and calcium-ATPase activity of plasma membranes from human myometrium and placental trophoblast. Hypertens Pregnancy 22:295–304

Cartwright JE, Fraser R, Leslie K, Wallace AE, James JL (2010) Remodelling at the maternal-fetal interface: relevance to human pregnancy disorders. Reproduction 140:803–813

Cetin I, Alvino G (2009) Intrauterine growth restriction: implications for placental metabolism and transport. A review. Placenta 30(suppl A):S77–S82

Chatterjee S, Mayor S (2001) The GPI-anchor and protein sorting. Cell Mol Life Sci 58:1969–1987

Chichili GR, Rodgers W (2007) Clustering of membrane raft proteins by the actin cytoskeleton. J Biol Chem 282:36682–36691

Danielsen EM, Hansen GH (2003) Lipid rafts in epithelial brush borders: atypical membrane microdomains with specialized functions. Biochim Biophys Acta 1617:1–9

De Gregorio N, Vallejos C, Berrios M, Riquelme G (2010) Potassium channels in human placenta from preeclamptic and IUGR preganacies: expression, function and association to lipid rafts. Placenta 31:A127

Dekker GA, Sibai BM (1998) Etiology and pathogenesis of pre-eclampsia: current concepts. Am J Obstet Gynecol 179:1359–1375

Diaz P, Vallejos C, Guerrero I, Riquelme G (2008) Barium, TEA and sodium sensitive potassium channels are present in the human placental syncytiotrophoblast apical membrane. Placenta 29:883–891

Fantini J, Garmy N, Mahfoud R, Yahi N (2002) Lipid rafts: structure, function and role in HIV, Alzheimer's and prion diseases. Expert Rev Mol Med 4:1–22

Gaus K, Rodriguez M, Ruberu KR, Gelissen I, Sloane TM, Kritharides L, Jessup W (2005) Domain-specific lipid distribution in macrophage plasma membranes. J Lipid Res 46:1526–1538

Godoy V, Riquelme G (2008) Distinct lipid rafts in subdomains from human placental apical syncytiotrophoblast membranes. J Membr Biol 224:21–31

Guller S, Ma YY, Fu HH, Krikun G, Abrahams VM, Mor G (2008) The placental syncytium and the pathophysiology of preeclampsia and intrauterine growth restriction: a novel assay to assess syncytial protein expression. Ann N Y Acad Sci 1127:129–133

Hanada K, Nishijima M, Akamatsu Y, Pagano RE (1995) Both sphingolipids and cholesterol participate in the detergent insolubility of alkaline phosphatase, a glycosylphosphatidylinositol-anchored protein, in mammalian membranes. J Biol Chem 270:6254–6260

Harder T, Gerke V (1994) The annexin II2p11(2) complex is the major protein component of the triton X-100-insoluble low-density fraction prepared from MDCK cells in the presence of Ca^{2+}. Biochim Biophys Acta 1223:375–382

Harder T, Scheiffele P, Verkade P, Simons K (1998) Lipid domain structure of the plasma membrane revealed by patching of membrane components. J Cell Biol 141:929–942

Huppertz B (2008) Placental origins of preeclampsia: challenging the current hypothesis. Hypertension 51:970–975

Huppertz B, Burton G, Cross JC, Kingdom JC (2006a) Placental morphology: from molecule to mother—a dedication to Peter Kaufmann—a review. Placenta 27(Suppl A):S3–S8

Huppertz B, Kadyrov M, Kingdom JC (2006b) Apoptosis and its role in the trophoblast. Am J Obstet Gynecol 195:29–39

Jahn KA, Braet F (2008) Monitoring membrane rafts in colorectal cancer cells by means of correlative fluorescence electron microscopy (CFEM). Micron 39:1393–1397

Jansson T, Scholtbach V, Powell TL (1998) Placental transport of leucine and lysine is reduced in intrauterine growth restriction. Pediatr Res 44:532–537

Jimenez V, Henriquez M, Llanos P, Riquelme G (2004) Isolation and purification of human placental plasma membranes from normal and pre-eclamptic pregnancies. A comparative study. Placenta 25:422–437

Johansson M, Karlsson L, Wennergren M, Jansson T, Powell TL (2003) Activity and protein expression of Na^+/K^+ ATPase are reduced in microvillous syncytiotrophoblast plasma membranes isolated from pregnancies complicated by intrauterine growth restriction. J Clin Endocrinol Metab 88:2831–2837

Jones CJ, Fox H (1980) An ultrastructural and ultrahistochemical study of the human placenta in maternal pre-eclampsia. Placenta 1:61–76

Juez G (1989) Intrauterine growth curve for the appropriate diagnosis of intrauterine growth retardation. Rev Med Chil 117:1311

Lichtenberg D, Goni FM, Heerklotz H (2005) Detergent-resistant membranes should not be identified with membrane rafts. Trends Biochem Sci 30:430–436

Lindheimer MD, Katz AI (1989) Preeclampsia: pathophysiology, diagnosis, and management. Annu Rev Med 40:233–250

Llanos P, Henriquez M, Riquelme G (2002) A low conductance, non-selective cation channel from human placenta. Placenta 23:184–191

Marin R, Riquelme G, Godoy V, Diaz P, Abad C, Caires R, Proverbio T, Pinero S, Proverbio F (2008) Functional and structural demonstration of the presence of Ca-ATPase (PMCA) in both microvillous and basal plasma membranes from syncytiotrophoblast of human term placenta. Placenta 29:671–679

Meder D, Moreno MJ, Verkade P, Vaz WL, Simons K (2006) Phase coexistence and connectivity in the apical membrane of polarized epithelial cells. Proc Natl Acad Sci USA 103:329–334

Mooseker MS (1985) Organization, chemistry, and assembly of the cytoskeletal apparatus of the intestinal brush border. Annu Rev Cell Biol 1:209–241

Morales FC, Takahashi Y, Kreimann EL, Georgescu MM (2004) Ezrin-radixin-moesin (ERM)-binding phosphoprotein 50 organizes ERM proteins at the apical membrane of polarized epithelia. Proc Natl Acad Sci USA 101:17705–17710

Morales B, Vallejos C, Riquelme G (2009) Canales de Cloruro en Sinciciotrofoblasto de Placentas con Restricción de Crecimiento Intrauterino (RCIU). R90

Muhlhauser J, Crescimanno C, Kasper M, Zaccheo D, Castellucci M (1995) Differentiation of human trophoblast populations involves alterations in cytokeratin patterns. J Histochem Cytochem 43:579–589

Nochy D, Hinglais N, Jacquot C, Gaudry C, Remy P, Bariety J (1986) De novo focal glomerular sclerosis in preeclampsia. Clin Nephrol 25:116–121

Norberg S, Powell TL, Jansson T (1998) Intrauterine growth restriction is associated with a reduced activity of placental taurine transporters. Pediatr Res 44:233–238

Paradela A, Bravo SB, Henriquez M, Riquelme G, Gavilanes F, Gonzalez-Ros JM, Albar JP (2005) Proteomic analysis of apical microvillous membranes of syncytiotrophoblast cells reveals a high degree of similarity with lipid rafts. J Proteome Res 4:2435–2441

Powers RW, Catov JM, Bodnar LM, Gallaher MJ, Lain KY, Roberts JM (2008) Evidence of endothelial dysfunction in preeclampsia and risk of adverse pregnancy outcome. Reprod Sci 15:374–381

Rajendran L, Simons K (2005) Lipid rafts and membrane dynamics. J Cell Sci 118:1099–1102

Rajendran L, Masilamani M, Solomon S, Tikkanen R, Stuermer CA, Plattner H, Illges H (2003) Asymmetric localization of flotillins/reggies in preassembled platforms confers inherent polarity to hematopoietic cells. Proc Natl Acad Sci USA 100:8241–8246

Riquelme G, Parra M (1999) Regulation of human placental chloride channel by arachidonic acid and other cis unsaturated fatty acids. Am J Obstet Gynecol 180:469–475

Riquelme G, Stutzin A, Barros LF, Liberona JL (1995) A chloride channel from human placenta reconstituted into giant liposomes. Am J Obstet Gynecol 173:733–738

Romanenko VG, Fang Y, Byfield F, Travis AJ, Vandenberg CA, Rothblat GH, Levitan I (2004) Cholesterol sensitivity and lipid raft targeting of Kir2.1 channels. Biophys J 87:3850–3861

Roos S, Powell TL, Jansson T (2004) Human placental taurine transporter in uncomplicated and IUGR pregnancies: cellular localization, protein expression, and regulation. Am J Physiol Regul Integr Comp Physiol 287:R886–R893

Schroeder RJ, Ahmed SN, Zhu Y, London E, Brown DA (1998) Cholesterol and sphingolipid enhance the Triton X-100 insolubility of glycosylphosphatidylinositol-anchored proteins by promoting the formation of detergent-insoluble ordered membrane domains. J Biol Chem 273:1150–1157

Sibley CP, Pardi G, Cetin I, Todros T, Piccoli E, Kaufmann P, Huppertz B, Bulfamante G, Cribiu FM, Ayuk P, Glazier J, Radaelli T (2002) Pathogenesis of intrauterine growth restriction (IUGR) conclusions derived from a European Union Biomed 2 Concerted Action project "Importance of oxygen supply in intrauterine growth restricted pregnancies"—a workshop report. Placenta 23(suppl A):S75–S79

Simons K, Ehehalt R (2002) Cholesterol, lipid rafts, and disease. J Clin Invest 110:597–603

Simons K, Toomre D (2000) Lipid rafts and signal transduction. Nat Rev Mol Cell Biol 1:31–39

Smith PK, Krohn RI, Hermanson GT, Mallia AK, Gartner FH, Provenzano MD, Fujimoto EK, Goeke NM, Olson BJ, Klenk DC (1985) Measurement of protein using bicinchoninic acid. Anal Biochem 150:76–85

Staneva G, Angelova MI, Koumanov K (2004) Phospholipase A2 promotes raft budding and fission from giant liposomes. Chem Phys Lipids 129:53–62

Taylor RN (1997) Review: immunobiology of preeclampsia. Am J Reprod Immunol 37:79–86

Than NG, Romero R, Hillermann R, Cozzi V, Nie G, Huppertz B (2008) Prediction of preeclampsia—a workshop report. Placenta 29(suppl A):S83–S85

Tyska MJ, Mackey AT, Huang JD, Copeland NG, Jenkins NA, Mooseker MS (2005) Myosin-1a is critical for normal brush border structure and composition. Mol Biol Cell 16:2443–2457

Vallejos C, Riquelme G (2007) The maxi-chloride channel in human syncytiotrophoblast: a pathway for taurine efflux in placental volume regulation? Placenta 28:1182–1191

Vallejos C, Morales B, Madrid G, Riquelme G (2010) Chloride channels in human syncytiotrophoblast apical and basal membrane from preeclamptic and IUGR pregnancies. Placenta 31:A128

van der Goot FG, Harder T (2001) Raft membrane domains: from a liquid-ordered membrane phase to a site of pathogen attack. Semin Immunol 13:89–97

Wald FA, Oriolo AS, Casanova ML, Salas PJ (2005) Intermediate filaments interact with dormant ezrin in intestinal epithelial cells. Mol Biol Cell 16:4096–4107

Widmer M, Villar J, Benigni A, Conde-Agudelo A, Karumanchi SA, Lindheimer M (2007) Mapping the theories of preeclampsia and the role of angiogenic factors: a systematic review. Obstet Gynecol 109:168–180

Wiechelman KJ, Braun RD, Fitzpatrick JD (1988) Investigation of the bicinchoninic acid protein assay: identification of the groups responsible for color formation. Anal Biochem 175:231–237

Xu W, Yoon SI, Huang P, Wang Y, Chen C, Chong PL, Liu-Chen LY (2006) Localization of the kappa opioid receptor in lipid rafts. J Pharmacol Exp Ther 317:1295–1306